CHEMISTRY
A EUROPEAN JOURNAL

DOI: 10.1002/chem.201000167

Structure-Based Design of Platinum(II) Complexes as c-*myc* Oncogene Down-Regulators and Luminescent Probes for G-Quadruplex DNA

Ping Wang,[a] Chung-Hang Leung,[a] Dik-Lung Ma,[a, b] Siu-Cheong Yan,[a] and Chi-Ming Che*[a]

Abstract: A series of platinum(II) complexes with tridentate ligands was synthesized and their interactions with G-quadruplex DNA within the c-*myc* gene promoter were evaluated. Complex **1**, which has a flat planar 2,6-bis(benzimidazol-2-yl)pyridine (bzimpy) scaffold, was found to stabilize the c-*myc* G-quadruplex structure in a cell-free system. An in silico G-quadruplex DNA model has been constructed for structure-based virtual screening to develop new Pt^{II}-based complexes with superior inhibitory activities. By using complex **1** as the initial structure for hit-to-lead optimization, bzimpy and related 2,6-bis(pyrazol-3-yl)pyridine (dPzPy) scaffolds containing amine side-chains emerge as the top candidates. Six of the top-scoring complexes were synthesized and their interactions with c-*myc* G-quadruplex DNA have been investigated. The results revealed that all of the complexes have the ability to stabilize the c-*myc* G-quadruplex. Complex **3a** ($[Pt^{II}$**L2R**$]^+$; **L2** = 2,6-bis[1-(3-piperidinepropyl)-1*H*-enzo[*d*]-imidazol-2-yl]pyridine, **R** = Cl) displayed the strongest inhibition in a cell-free system (IC_{50} = 2.2 μM) and was 3.3-fold more potent than that of **1**. Complexes **3a** and **4a** ($[Pt^{II}$**L3R**$]^+$; **L3** = 2,6-bis[1-(3-morpholinopropyl)-1*H*-pyrazol-3-yl]pyridine, **R** = Cl) were found to effectively inhibit c-*myc* gene expression in human hepatocarcinoma cells with IC_{50} values of ≈17 μM, whereas initial hit **1** displayed no significant effect on gene expression at concentrations up to 50 μM. Complexes **3a** and **4a** have a strong preference for G-quadruplex DNA over duplex DNA, as revealed by competition dialysis experiments and absorption titration; **3a** and **4a** bind G-quadruplex DNA with binding constants (K) of approximately 10^6–10^7 $dm^3 mol^{-1}$, which are at least an order of magnitude higher than the K values for duplex DNA. NMR spectroscopic titration experiments and molecular modeling showed that **4a** binds c-*myc* G-quadruplex DNA through an external end-stacking mode at the 3′-terminal face of the G-quadruplex. Intriguingly, binding of c-*myc* G-quadruplex DNA by **3b** is accompanied by an increase of up to 38-fold in photoluminescence intensity at λ_{max} = 622 nm.

Keywords: DNA structures · G-quadruplexes · ligand effects · oncogenes · platinum

Introduction

DNA is the molecular target for an array of antitumor[1,2] and antimicrobial drugs.[3] The design and development of new drugs that target specific DNA secondary structures or sequences continues to be a challenge. Guanine-rich DNA sequences can form four-stranded secondary structures called G-quadruplexes, which are stabilized by Hoogsteen hydrogen bonds between four guanines.[4] G-quadruplexes have aroused considerable interest in medicinal chemistry because they represent alternative DNA structures that can potentially be targeted by small molecules. Thus, the stabilization of G-quadruplex structures in the promoter region of oncogenes is an emerging field in the design of anticancer drugs.

Particular emphasis has been focused on the c-*myc* oncogene, which plays a non-trivial role in many cellular events. The overexpression of the c-*myc* oncogene is linked with cellular proliferation and inhibition of differentiation, leading to its association with a wide range of human cancers.[5–8] Transcriptional control of c-*myc* has emerged as an attractive target for anticancer therapeutic strategies. The c-*myc* oncogene contains parallel-stranded quadruplexes in the nu-

[a] P. Wang, Dr. C.-H. Leung, Dr. D.-L. Ma, Dr. S.-C. Yan, Prof. C.-M. Che
Department of Chemistry and Open Laboratory of Chemical Biology of the Institute of Molecular Technology for Drug Discovery and Synthesis
The University of Hong Kong
Pokfulam Road, Hong Kong (P.R. China)
Fax: (+852) 2857-1586
E-mail: cmche@hku.hk

[b] Dr. D.-L. Ma
Current address: Department of Chemistry
Hong Kong Baptist University
Kowloon Tong, Hong Kong (P.R. China)

Supporting information for this article is available on the WWW under http://dx.doi.org/10.1002/chem.201000167.

clease hypersensitivity element (NHE) III_1 that is upstream of the P1 and P2 promoters.[9–11]

The transcription of c-*myc* can be inhibited by the stabilization of G-quadruplexes by using specific G-quadruplex binders. Since the first report on the interaction between small molecules and G-quadruplex DNA in 1997,[12] a variety of G-quadruplex binders have been described, such as telomestatin, TMPyP4 (*meso*-5,10,15,20-tetrakis-(*N*-methyl-4-pyridyl)porphine), Se2SAP (5,10,15,20-[tetra(*N*-methyl-3-pyridyl)]-26,28-diselenasapphyrin chloride), perylenes, quindolines, and berberine.[13–29] However, metal complexes only represent a small fraction of the reported G-quadruplex binders.[20–29] Notable examples include a manganese(III) porphyrin developed by Pratviel and co-workers that is 10000-fold more selective for G-quadruplex DNA than for duplex DNA,[22b] and square-planar nickel(II) salphen (H_2salphen = *N*,*N*′-bis(salicylidene)-1,2-phenylenediamne) complexes reported by Neidle and co-workers.[27] Our group has recently reported that platinum(II) complexes containing Schiff-base ligands could function as selective luminescent probes for G-quadruplex DNA and down-regulate c-*myc* oncogene expression in vitro.[28b] More recently, Luedtke and co-workers[29] reported that tetrakis(diisopropylguanidinio)zinc(II) phthalocyanine could also function as high-affinity G-quadruplex fluorescent probes and transcriptional regulators.

The reported G-quadruplex binders generally comprise a planar aromatic scaffold to bind to guanine tetrads and with appended side-chains to enhance the binding interaction.[17,25a,27a] We predict that platinum(II) complexes with structures as depicted in Figure 1 could be developed into effective G-quadruplex binders. The rationale is to maintain the planar π-conjugation of the 2,6-bis(benzimidazol-2-yl)-pyridine (bzimpy) or 2,6-bis(pyrazol-3-yl)pyridine (dPzPy) scaffolds through the formation of platinum(II) complexes to enable π–π interactions with the G-quartet. The appended side-chains could improve water solubility and increase potential interactions with G-quadruplex loops and grooves. Compared with the Schiff-base complexes reported in our previous work,[28b] complexes **1**–**4** have the following advantages: 1) these complexes are cationic, which could lead to stronger interactions with the negatively charged sugar–phosphate backbone of DNA; 2) these complexes have a more extended π-conjugated planar aromatic structure, which could enhance π–π interactions with the G tetrads; and 3) the two scaffolds bzimpy and dPzPy allow attachment of side-chains in different directions, which allows for more structural diversity. Furthermore, these platinum(II) complexes with π-conjugated aromatic ligands can act as luminescent probes for G-quadruplex DNA due to the photoluminescent properties of transition-metal complexes being sensitive to the local environment.[28–31] They are non-emissive in aqueous solution due to non-radiative decay of the excited state by complex–solvent interactions, but fluoresce strongly when bound to DNA.

In this work, we employed the cell-free polymerase stop assay for initial screening of platinum(II) complexes for G-quadruplex DNA stabilization activity. Complex **1**, with a flat planar bzimpy scaffold, was found to stabilize the c-*myc* G-quadruplex structure. Encouraged by this result, we used complex **1** as the initial hit for optimization through docking-based virtual screening of over 550 platinum(II) complexes (Figure S1, Supporting Information) to develop new platinum(II) bzimpy complexes with superior inhibitory activities. The intramolecular G-quadruplex loop isomer of NHE III_1 was constructed by using the X-ray crystal structure of the intramolecular human telomeric G-quadruplex DNA (PDB code: 1KF1)[32] as a model to develop a high-throughput screening platform for complexes that bind to G-quadruplex DNA. The hit-to-lead optimization process by using virtual screening led to platinum(II) complexes **2**–**3**, which contain bzimpy ligands with appended amine side-chains, and platinum(II) complex **4** based on the related dPzPy scaffold. These complexes were synthesized and tested in both cell-free and cell-based assays for G-quadruplex

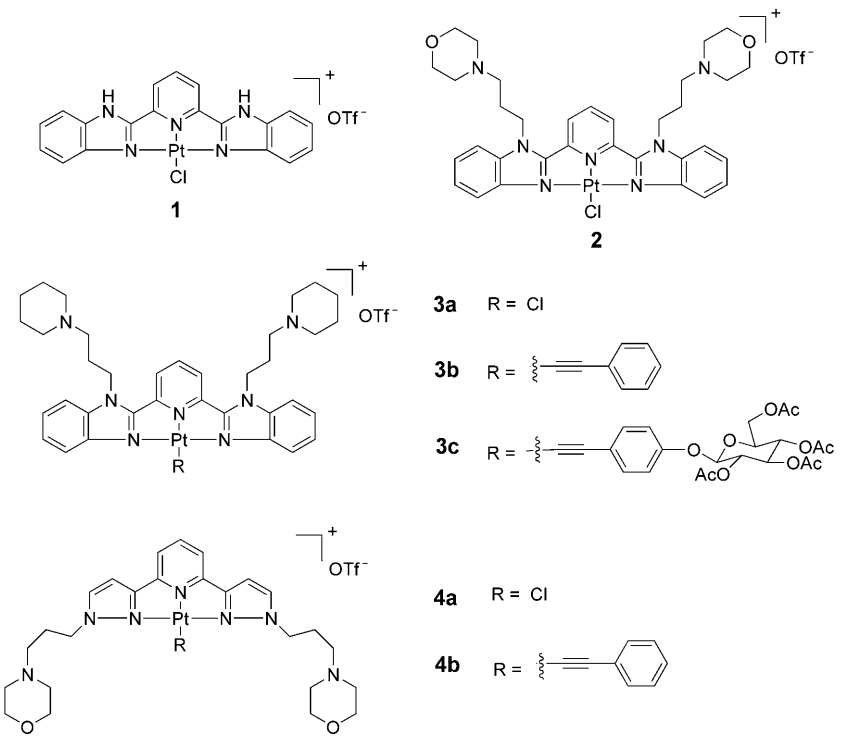

Figure 1. Structures of complexes **1**–**4**.

stabilization activity. We demonstrate herein that these platinum(II) complexes with amino side-chains on the bzimpy or dPzPy scaffolds can effectively stabilize G-quadruplex and down-regulate c-*myc* expression in human hepatocarcinoma HepG2 cells. The biological activities of optimized complexes **2**–**4** are superior to those of initial hit complex **1**, which demonstrates the effective application of in silico molecular modeling in improving the potency of biologically active compounds. Furthermore, these complexes are more potent than the Schiff-base platinum(II) complexes previously reported by our group.

Results

Ligands 2,6-bis(benzimidazol-2-yl)pyridine (bzimpy)[33] and 2,6-bis(pyrazol-3-yl)pyridine (dPzPy)[34] were synthesized according to reported procedures. The amine side-chains were prepared from morpholine or piperidine through a Michael addition to methyl acrylate, followed by reduction by lithium aluminium hydride and chlorination with SO_2Cl_2. The amine side-chains were introduced to bzimpy and dPzPy to afford the ligands 2,6-bis[1-(3-morpholinopropyl)-1*H*-benzo[*d*]imidazol-2-yl]pyridine (**L1**), 2,6-bis[1-(3-piperidinepropyl)-1*H*-benzo[*d*]imidazol-2-yl]pyridine (**L2**), and 2,6-bis[1-(3-morpholinopropyl)-1*H*-pyrazol-3-yl]pyridine (**L3**). Complexes **1**, **2**, **3a**, and **4a** were synthesized by treating ligands bzimpy, **L1**, **L2**, and **L3** with $[Pt(DMSO)_2Cl_2]$ under similar conditions. Complexes **3a** and **4a** were further converted to phenylethynyl-substituted complexes **3b**, **3c**, and **4b** by reported procedures. Based on UV/Vis absorption and NMR spectroscopic measurements, these platinum(II) complexes are stable in aqueous solutions for 48 h at room temperature.

Spectroscopic properties: The UV/Vis absorption spectrum of **1** in H_2O/DMSO shows two intense absorption bands at $\lambda_{max}=385$ ($\varepsilon\approx1.1\times10^4$ dm^{3}mol^{-1}cm^{-1}) and 412 nm ($\varepsilon\approx0.5\times10^4$ dm^{3}mol^{-1}cm^{-1}). With reference to previous studies,[35] the absorption bands at $\lambda=385$–412 nm are assigned to metal-to-ligand charge transfer (MLCT) and ligand-to-ligand charge transfer (LLCT) transitions. The absorption spectra of complexes **2**–**4** are similar to that of **1** in the spectral region of $\lambda=280$–450 nm, and are solvent sensitive. For example, the low-energy broad absorption band of **3a** is redshifted in energy in low-polarity solvents, for example, in MeOH $\lambda_{max}=413$, 430 nm and in CH_3CN $\lambda_{max}=414$, 432 nm. As the solvent polarity decreases, for example, on going from methanol to acetonitrile, the low-energy absorption bands redshift in energy and the emission λ_{max} is slightly redshifted from $\lambda=634$ to 637 nm. The negative solvatochromic shift reveals that the ground state is more polar than the excited state. The UV/Vis absorption spectra of **1**–**4** are given in the Supporting Information, and the spectral data recorded in various solutions are summarized in Table 1.

Excitation of **1** (50 μM in CH_3CN) at $\lambda=350$ nm gives an emission at $\lambda=623$ nm. The emission lifetime of **1** is 0.3 μs and the emission quantum yield (Φ) is 0.06 in CH_3CN. The emission maxima of complexes **2**, **3a**, and **3b** in CH_3CN are at $\lambda=640$ ($\Phi=0.05$, $\tau=0.6$ μs), 637 ($\Phi=0.04$, $\tau=0.6$ μs), and 638 nm ($\Phi=0.06$, $\tau=1.5$ μs), respectively, whereas complexes **4a** and **4b** in CH_3CN display emission maxima at $\lambda=613$ ($\Phi=0.10$, $\tau=3.10$ μs) and 619 nm ($\Phi=0.24$, $\tau=1.6$ μs), respectively. Emission in H_2O (containing 5% DMSO) solution was only observed for complexes **1**, **2**, **3b**, and **4a**, whereas the emissions of **3a** and **4b**, which are presumed to be MLCT in nature, are quenched in aqueous solution. The photophysical data of **1**–**4** are summarized in Table 1.

Table 1. Photophysical data of **1**–**4** in various solvents at 298 K.

	Medium[a]	λ_{abs} [nm]	ε [$\times10^4$ dm^{3}mol^{-1}cm^{-1}]	$\lambda_{em(max)}$ [nm]	τ [μs] (Φ_{em})
1	H_2O/DMSO	245, 261, 315, 385, 412	1.61, 0.95, 1.7, 1.1, 0.5	628	0.2 (0.04)
	CH_3CN	313, 336, 356, 369, 414, 436	2.1, 1.86, 1.63, 1.73, 0.42, 0.33	623	0.3 (0.06)
	MeOH	241, 330, 358, 367, 413, 430	1.38, 1.16, 1.18, 1.2, 0.45, 0.38	565	<0.1 (0.05)
2	H_2O/DMSO	240, 329, 367, 384, 404, 414	0.92, 1.10, 1.21, 0.66, 0.39, 0.26	668	0.4 (0.03)
	CH_3CN	312, 338, 363, 375, 415, 432	1.40, 1.41, 1.32, 1.25, 0.38, 0.23	640	0.6 (0.05)
	MeOH	310, 336, 352, 361, 412, 426	1.43, 1.28, 1.29, 1.13, 0.47, 0.17	638	0.4 (0.04)
3a	H_2O/DMSO	312, 342, 376, 404, 425	1.56, 1.48, 1.12, 0.45, 0.28	Non-emissive	
	CH_3CN	247, 313, 347, 370, 414, 432	1.24, 1.67, 1.70, 1.46, 0.32, 0.25	637	0.6 (0.04)
	MeOH	313, 341, 356, 369, 413, 430	1.63, 1.61, 1.53, 1.37, 0.25, 0.1	634	0.7 (0.04)
3b	H_2O/DMSO	273, 328, 422, 465	1.91, 1.81, 0.39, 0.22	641	1.1 (0.05)
	CH_3CN	246, 326, 352, 424	4.03, 2.17, 2.1, 0.38	638	1.5 (0.06)
	MeOH	245, 325, 352, 420	2.32, 1.61, 1.63, 0.18	Non-emissive	
3c	H_2O/DMSO	274, 327, 421	2.39, 1.81, 0.22	n.d.[b]	
	CH_3CN	270, 325, 424	3.56, 1.87, 0.29	n.d.[b]	
	MeOH	269, 324, 423	2.31, 1.81, 0.21	n.d.[b]	
4a	H_2O/DMSO	264, 287, 316, 330, 392, 412	1.62, 1.28, 0.83, 0.86, 0.24, 0.1	617	2.2 (0.06)
	CH_3CN	262, 285, 317, 330, 388, 422	1.47, 1.13, 0.81, 0.85, 0.21 ,0.14	613	3.1 (0.10)
	MeOH	264, 283, 316, 330, 384, 414	1.62, 1.28, 0.83, 0.85, 0.26, 0.15	Non-emissive	
4b	H_2O/DMSO	259, 324, 393, 412, 430	3.91, 2.0, 0.33, 0.24, 0.18	Non-emissive	
	CH_3CN	286, 317, 330, 408, 453	1.15, 0.82, 0.85, 0.25, 0.1	619	1.6 (0.24)
	MeOH	258, 328, 386, 407, 444	3.61, 1.44, 0.45, 0.27, 0.1	616	1.3 (0.2)

[a] H_2O/DMSO 95:5 v/v. [b] Not determined.

Polymerase stop assay: To investigate the ability of complex **1** to stabilize c-*myc* G-quadruplex, a polymerase stop assay was performed by using the single-stranded G4A1 c-*myc* DNA sequence (5′-TGGGGAGGGTGGGGAGGGTGGG-GAAGG-3′). The specific binding of the complex with intramolecular G-quadruplex structures in G4A1 is expected to inhibit the action of the DNA polymerase.[15,17a] Complex **1** could stabilize a pre-formed G-quadruplex structure. The hybridization of G4A1 with a complementary strand (5′-ATCGATCGCTTCTCGTCCTTCCCCA-3′) overlapping the last G repeat was blocked. The polymerase chain reaction (PCR) and formation of the final 43 bp double-stranded DNA PCR product were inhibited (Figure 2).

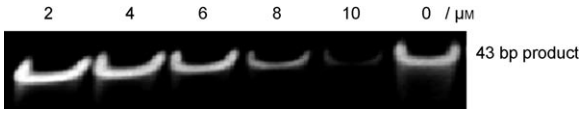

Figure 2. Dose-dependent inhibition of G4A1 PCR amplification by **1**, presumably through stabilization of the G-quadruplex structure.

Molecular modeling for complex 1: To gain further insight into the binding mode of complex **1**, we performed molecular modeling with the NHE III_1 intramolecular G-quadruplex loop isomer model. The biologically relevant G-quadruplexes exist as a mixture of four different loop isomers, of which the 1:2:1 isomer is predominant.[36a] The folding pattern of this parallel G-quadruplex structure has also been defined by NMR spectroscopy.[36b] Because nucleotides G2–G5 in the G4A1 DNA sequence (5′-TGGGGAGGGTGGGGAGGGTGGGGAAGG-3′) are not involved in the G-quartet structure, a truncated 18 bp sequence (5′-AGGGTGGGGAGGGTGGGG-3′) was used as a model for the present work. In this binding mode, **1** is stacked on the ends of G-quadruplex at the GT quadruplex terminus, close to the 3′-terminal face of the G-quadruplex with a calculated binding energy of $-53\,kcal\,mol^{-1}$ (Figure 3). In addition, the unfavorable binding energy of $+32\,kcal\,mol^{-1}$ calculated for the intercalation binding sites suggests that the interaction between **1** and G-quadruplex DNA should not be intercalative in nature. Thus, **1** is a useful scaffold for developing new platinum(II) complexes with improved inhibitory activity against c-*myc* transcription.

Lead optimization: To develop new lead analogues with improved potency and specificity against c-*myc* transcription, a structure-guided parallel synthesis concept was adopted by using computer-aided drug design. Molecular modeling permits rapid screening of multiple analogues, facilitating preselection of a subset of furnished analogues with favorable binding affinities. In this approach, the bzimpy scaffold was modified on the basis of receptor structural information. By using the mode of binding of the platinum(II) complex **1** with the G-quadruplex DNA as the template for lead optimization, we were hoping to expedite the discovery of derivatives of **1** with greater specificity and selectivity towards the G-quadruplex structure of c-*myc*.

By employing **1** as the structural template, more than 550 platinum(II) complexes containing tridentate ligands and different amine side-chains designed for intramolecular G-quadruplex DNA interaction were screened in silico (Figure S1, Supporting Information). Each platinum(II) complex was docked onto a grid representation of the receptor and a score was assigned to each complex to reflect the quality of the interaction according to the ICM method (Molsoft).[37] Analysis of the conformation energy of all the Pt^{II} complexes revealed that the side-chains are able to bury deeply into the G-quadruplex DNA grooves and make several electrostatic and hydrogen-bonding contacts. Complex **4a** ($[Pt^{II}\mathbf{L3R}]^+$, **L3** = 2,6-bis[1-(3-morpholinopropyl)-1*H*-pyrazol-3-yl]pyridine, **R** = Cl) was identified as the top-scoring molecule through virtual screening (Figure 4). Subsequently,

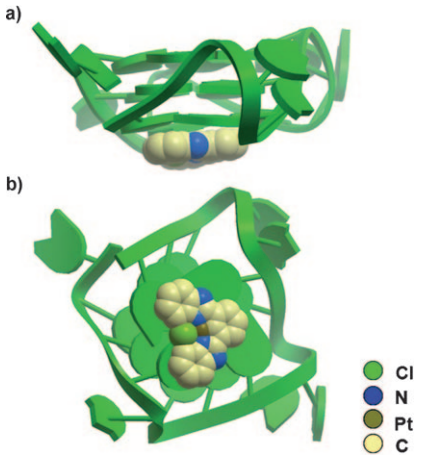

Figure 3. Schematic diagram showing a) a side view and b) a top view of the interactions between **1** and the G-quadruplex structure of c-*myc*. The G-quadruplex and **1** are shown in ribbon and space-filling representations, respectively.

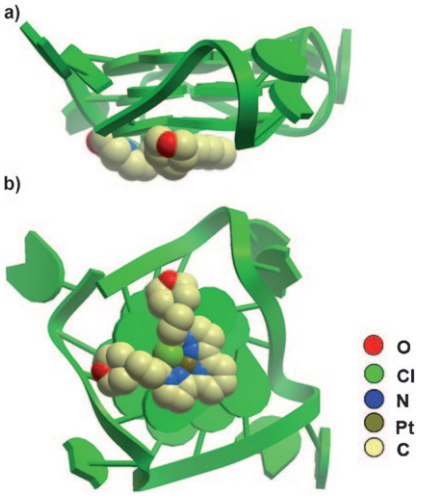

Figure 4. Schematic diagram showing a) a side view and b) a top view of the interactions between **4a** and the G-quadruplex structure of c-*myc*. The G-quadruplex and **4a** are shown in ribbon and space-filling representations, respectively.

six of the top scoring complexes **2**–**4** were synthesized and tested experimentally for G-quadruplex selectivity and their ability to inhibit c-*myc* gene promoter activity in cell-free systems and c-*myc* expression in cultured cells. Notably, we observed that complexes **2**, **3a**, and **4a** were found to display superior selectivity for G-quadruplex DNA over duplex DNA, and exhibited significant stabilization of G-quadruplex and down-regulation of c-*myc* oncogene expression (see below).

Absorption titration: The interaction of lead complexes **2**, **3a**, **3b**, and **4a** with G-quadruplex DNA was first evaluated by UV/Vis absorption titration experiments. An intramolecular c-*myc* G-quadruplex structure was prepared by incubating oligonucleotide G4A1 in Tris/KCl buffer (Tris = tris(hydroxymethyl)aminomethane) at 95 °C for 10 min and cooling to room temperature overnight.[38] Aliquots of a millimolar stock G4A1 solution were added to the solution of platinum(II) complex and the absorption spectra were recorded in the range of $\lambda = 200$–550 nm after equilibration for 10 min per aliquot addition until the saturation point was reached. As shown in Figure 5, the addition of G4A1 quadruplex to a solution of **3a** in a Tris/KCl buffer led to a 7% hypochromism at $\lambda = 310$ nm in the UV/Vis spectrum without significant bathochromic spectral shift. By using a plot of $D/\Delta\varepsilon_{ap}$ versus D (Figure 5, bottom) according to the Scatchard equation,[39] the binding constant K of **3a** with G-quadruplex was calculated to be $(1.7 \pm 0.2) \times 10^7\ dm^3\,mol^{-1}$ at 20.0 °C. The K values for **2**, **3b**, and **4a** were similarly determined to be $\approx 10^6\ dm^3\,mol^{-1}$. To examine the binding specificity, the interaction between the complexes and duplex DNA was also investigated by UV titration. As summarized in Table 2, all complexes bind to calf thymus DNA (ct-DNA) with K values of 10^4–$10^5\ dm^3\,mol^{-1}$. The results indicate that the complexes show stronger binding to G-quadruplex DNA than to duplex DNA by at least one order of magnitude.

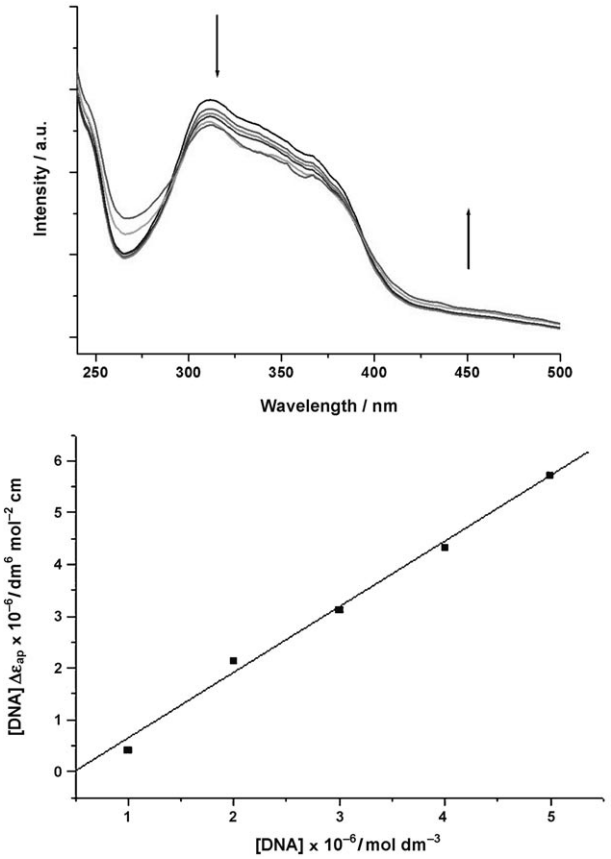

Figure 5. Top: UV/Vis spectra of **3a** (50 μM) in Tris/KCl buffer (100 mM KCl, 10 mM Tris/HCl, pH 7.5) with increasing amounts of oligonucleotide G4A1 at 20.0 °C ([G4A1-quadruplex]/[Pt] = 0–0.8). Bottom: Plot of $D/\Delta\varepsilon_{ap}$ vs. D.

Table 2. Binding constants of platinum(II) complexes upon addition of G4A1 quadruplex DNA and ct-DNA.

	K at 20 °C [$dm^3\,mol^{-1}$]	
	G4A1 quadruplex	ct-DNA
2	$(7.6\pm0.3)\times10^6$	$(1.1\pm0.1)\times10^5$
3a	$(1.7\pm0.2)\times10^7$	$(4.78\pm0.2)\times10^4$
3b	$(1.8\pm0.4)\times10^6$	$(7.52\pm0.4)\times10^4$
4a	$(3.1\pm0.2)\times10^6$	$(4.0\pm0.1)\times10^4$

UV melting study: To further study the effect of the platinum(II) complexes on the thermal stability of G4A1 quadruplex DNA, we monitored the melting profile at $\lambda =$ 295 nm. In the absence of Pt^{II} complex, the DNA melting temperature (T_m) of the G4A1 quadruplex in Tris/KCl buffer is 54.5 °C. Upon treatment of the G-quadruplex with the Pt^{II} complexes, T_m increases by 9.0–14.0 °C (Table 3), which indicates that the complexes improve the stability of the G-quadruplex structure, consistent with the high binding constants of the complexes for G-quadruplex DNA. The addition of complex **4a** leads to the highest T_m (Figure S18), revealing the strongest interaction with G-quadruplex DNA. This is consistent with the results of molecular docking studies showing that **4a** has the most favorable binding energy.

Table 3. Melting temperature (T_m) of G-quadruplex DNA obtained by monitoring absorbance at $\lambda = 295$ nm.

Complex	T_m [°C]	ΔT_m [°C]
DNA	54.5	–
DNA + **2**	63.5	9.0
DNA + **3a**	67.0	12.5
DNA + **3b**	66.0	11.5
DNA + **4a**	68.5	14.0

Competition dialysis: To further evaluate the selectivity of platinum(II) complexes **2**, **3a**, and **4a** for G-quadruplex over duplex DNA structures, we performed a competitive dialysis experiment by using G4A1 quadruplex oligomer and ct-DNA. In this assay, the nucleic acids were simultaneously dialyzed against a free ligand solution. A higher binding affinity was reflected by the higher concentration of metal

complex accumulated in the dialysis tube containing the specific form of DNA. As shown in Figure 6, the amount of bound complex for ct-DNA in the cases of complexes **2**, **3a**, and **4a** was nearly four- to eight-fold lower than that for G4A1-quadruplex DNA. This indicates that complexes **2**, **3a**, and **4a** are selective towards binding G-quadruplex DNA. Complex **3a** shows the highest selectivity for G-quadruplex DNA over duplex DNA, which is consistent with the results of absorption titration studies that **3a** has the highest *K* value.

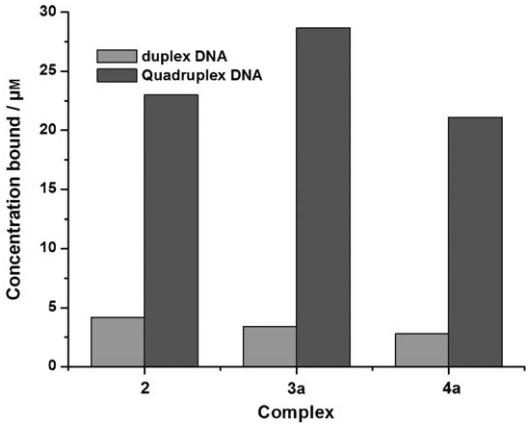

Figure 6. Results of the competition dialysis experiment. Solutions of the complexes were dialyzed against G4A1 quadruplex and ct-DNA for 24 h.

NMR spectroscopy: To investigate the binding mode of complex **4a**, we performed ^{1}H NMR spectroscopy experiments to monitor the interaction of complex **4a** with the G-quadruplex. A G4A3 quadruplex (5′-TGAGGGTGGIGAGGGTGGGGAAGG-3′) with clearly assigned G-tetrad imino proton signals (see ref. [40]) was used for this experiment. Upon addition of complex **4a** to a solution of G4A3 quadruplex (1.0 mM) at a [G4A3 quadruplex]/[**4a**] ratio of 1:1, the G5/G14 and G20 imino proton signals experienced the largest shift, revealing that **4a** binds closely to the 3′-terminal face of the G-quadruplex DNA (Figure 7). The changes in chemical shifts are similar to those displayed by daunomycin,[40] which is known to bind to G-quadruplexes. Thus, the ^{1}H NMR spectroscopy experiments provide additional evidence that **4a** binds externally to the stacks of guanine quartets within a quadruplex rather than intercalating between the stacks.

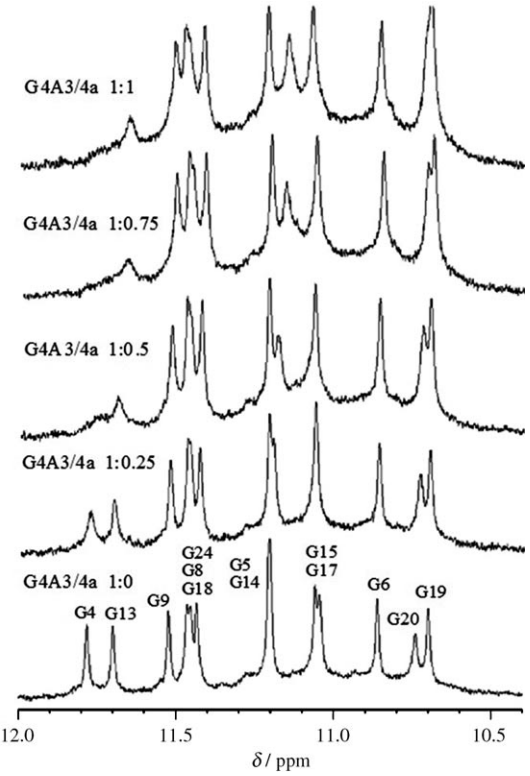

Figure 7. NMR spectroscopic titration of G4A3 quadruplex with **4a** at various ratios ([**4a**]/[G4A3] = 0, 0.25, 0.5, 0.75, and 1.0) in H_2O/D_2O (90:10) with KCl (150 mM), KH_2PO_4 (25 mM), EDTA (1 mM; pH 7.0). Only imino proton signals are shown (600 MHz, 25 °C).

Effect of the Pt^{II} complexes on the formation of c-*myc* G-quadruplex and c-*myc* expression: The induction and/or stabilization of a biologically relevant G-quadruplex by complexes **2**–**4b** were examined. As shown in Figure 8, all of the complexes dose-dependently stabilize the G-quadruplex in G4A1 as determined by the polymerase stop assay. The IC_{50} values were estimated to be 2.2–31.1 μM (Table 4). Complexes **3b**, **3c**, and **4b**, which have a coordinated phenylethynyl ligand as the R group, exhibited weaker inhibitory effect compared to complexes **3a** and **4a**. A parallel experiment was performed by using the oligomer G4A2 (5′-TGGGGAGGGTGGAAAGGGTGGGGAAGG-3′), which cannot form a G-quadruplex structure. No inhibition was observed for any of the platinum(II) complexes under this

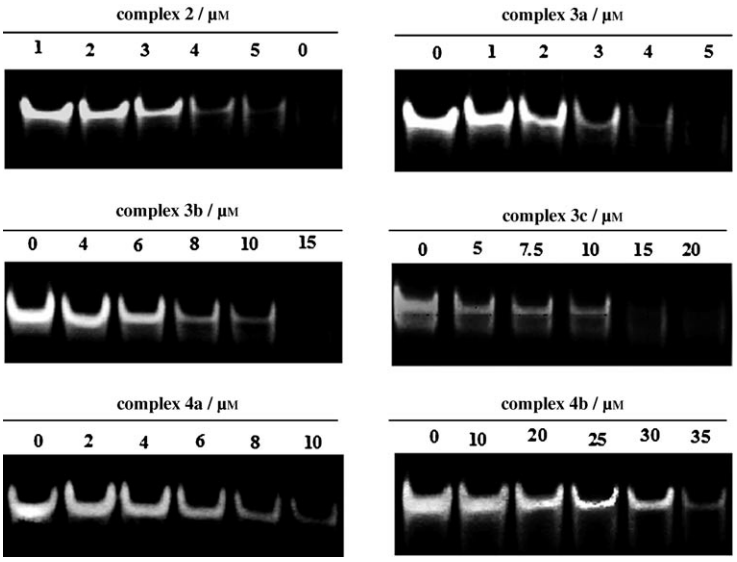

Figure 8. Dose-dependent inhibition of G4A1 PCR amplification by **2**–**4**.

Table 4. The estimated IC_{50} values of **1**–**4** based on the polymerase stop assay.

	IC_{50} [μM]
1	7.4
2	2.6
3a	2.2
3b	7.4
3c	13.8
4a	6.5
4b	31.1

condition, even at a complex concentration of 50 μM (Figure 9), which suggests that the inhibition of the PCR by the platinum(II) complexes required the formation of the G-quadruplex structure.

A reverse transcriptase–polymerase chain reaction (RT-PCR) was performed to determine the impact of complexes **1**, **2**, **3a**, and **4a** on the mRNA level of c-*myc* oncogene in HepG2 cells. Complexes **3a** and **4a** were equally potent against the transcription of c-*myc* ($IC_{50} \approx 17$ μM, Figure 10), whereas complex **2** moderately inhibited gene expression

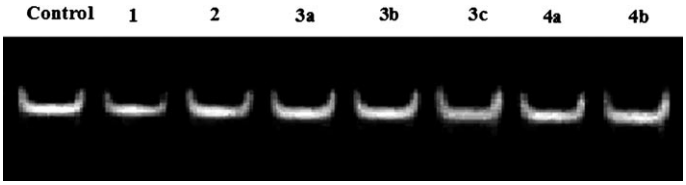

Figure 9. Complexes **1**–**4** (50 μM) have no significant effect on the PCR amplification of non-G-quadruplex G4A2 oligomers.

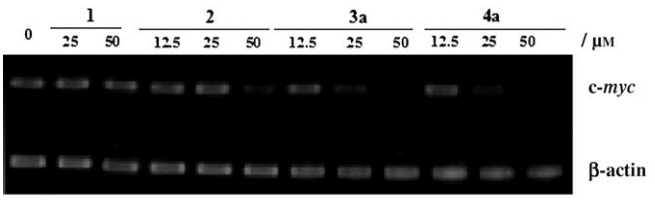

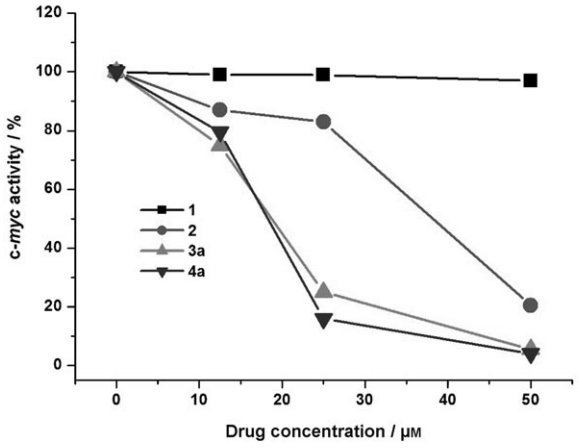

Figure 10. Top: A RT-PCR assay revealed dose-dependent inhibition of c-*myc* transcription by complexes **2**, **3a**, and **4a** but not **1** in HepG2 cells. Bottom: Relative c-*myc* expression level was measured by using a densitometer.

with an estimated IC_{50} value of ≈40 μM. However, complex **1** did not suppress the c-*myc* mRNA level at concentrations up to 50 μM.

Cytotoxicity test: By using an MTT assay, the cytotoxicities of **1**, **2**, **3a**, and **4a** against HeLa (human cervical epithelioid carcinoma), HepG2 (human hepatocarcinoma), and SUNE1 (human nasopharyngeal carcinoma) cancer cell lines were determined, whereas toxicity to normal cells was evaluated by using the normal lung fibroblast cell line CCD-19Lu. Complexes **1**, **2**, **3a**, and **4a** displayed moderate cytotoxicity against cancer cells after 8 days, but were less cytotoxic towards the normal cells (Table 5).

Table 5. Cytotoxicities of **1**–**4** towards three carcinoma cell lines (HeLa, HepG2, and SUNE1) and one normal human cell line (CCD-19Lu).[a]

	IC_{50} [μM]			
	HeLa	HepG2	SUNE1	CCD-19Lu
1	15.4±0.5	23.0±0.8	20.0±1.0	51.7±1.1
2	42.9±1.0	52.4±0.6	48.7±1.3	85.7±3.2
3a	57.2±1.2	61.3±1.7	49.9±0.9	93.2±7.6
4a	55.1±0.4	58.3±1.3	54.5±0.8	97.8±6.2

[a] Incubated for 8 d.

Emission titration: The binding of metal complexes to DNA can be assessed by emission spectroscopy. Complex **3b** is weakly emissive in aqueous Tris/KCl buffer solution at 20.0 °C. However, in the presence of G4A1, complex **3b** displays an intense photoluminescence at $\lambda_{max} = 622$ nm. As depicted in Figure 11, the addition of G4A1 to a solution of **3b** resulted in an increase in emission intensity of up to 38-fold when the concentration ratio of [G4A1]/[**3b**] was increased from 0 to 0.5. Importantly, when the emission titration experiment of **3b** was performed with ct-DNA (Figure S19, Supporting Information), only a 4.4-fold emission

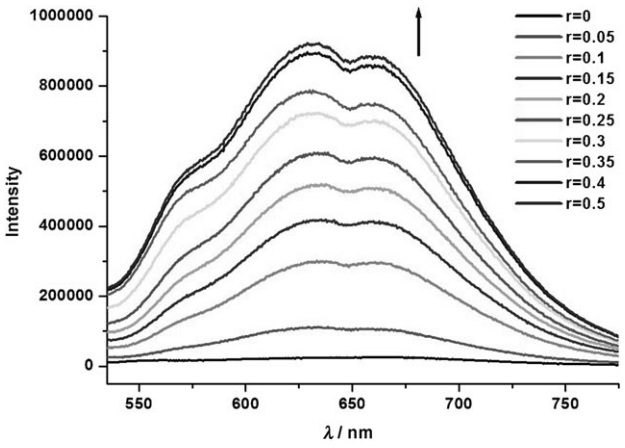

Figure 11. Emission spectra of **3b** (50 μM) in Tris/HCl buffer (10 mM, pH 7.4) containing KCl buffer (100 mM) with an increasing ratio of [G4A1]/[**3b**] = 0–0.5 at 20 °C.

enhancement was observed, revealing that complex **3b** is selective for G-quadruplex over duplex DNA.

Discussion

The c-*myc* oncogene acts as both a transcriptional activator and repressor, and the overexpression of this oncogene is related to increased cellular proliferation in a variety of malignant tumors, including breast, colon, cervix, small-cell lung, osteosarcomas, glioblastomas, and myeloid leukemias.[5–8] A guanine-rich region upstream of the P1 promoter of c-*myc* controlling 85 to 90% of the transcriptional activation of this gene can form an intramolecular G-quadruplex that functions as a transcriptional repressor element. Thus, modulating the transcription of c-*myc* through the G-quadruplex structure has emerged as an attractive target for anticancer therapeutic strategies. Some organic compounds have been reported to bind to and stabilize G-quadruplexes resulting in down-regulation of c-*myc*.[13–17] Our group has previously developed platinum(II) Schiff-base complexes that could stabilize G-quadruplex DNA structures and lead to down-regulation of c-*myc* oncogene expression.[28b] In this study, a series of platinum(II) complexes with bzimpy and dPzPy scaffolds, which are more planar than the Schiff-base scaffold, were synthesized and screened for their activities to induce or stabilize the c-*myc* G-quadruplex structures and to inhibit c-*myc* expression.

Lead optimization by using in silico virtual screening: The impetus for the development of the series of platinum(II) complexes used in this study was the initial discovery of complex **1** as a stabilizer of G-quadruplex DNA. We reasoned that the planar bzimpy scaffold was suited to end-stacking of the G-quadruplex structure, and that the introduction of side-chains could improve the binding affinity and selectivity of the metal complexes. By using **1** as the template for molecular modeling, we screened over 550 related platinum(II) complexes for G-quadruplex binding ability. The in silico molecular docking results show that platinum(II) complexes containing bzimpy or dPzPy scaffolds optimally interact with the c-*myc* G-quadruplex through stacking interactions at one end of the G-quadruplex structure. Because the Pt^{II} center in these complexes is positioned at the center of the quartet (surface of G-quadruplex ion channel), the side-chains introduced to the planar core of the molecule can increase the strength of the interaction between planar π-conjugated molecules and G-quadruplex DNA through formation of secondary interactions.[17,25a,27a] We have demonstrated that attaching the amino side-chains to the bzimpy or dPzPy scaffold led to an improvement in the biological activity, validating our molecular docking. The most effective complex, **4a**, displays high selectivity for the c-*myc* G-quadruplex over double-stranded DNA, and can significantly suppress c-*myc* transcription probably through the inhibition of c-*myc* gene promoter activity.

Rationalization of the selectivity of 4a: Hurley and co-workers showed that the biologically relevant parallel c-*myc* G-quadruplexes can exist as a mixture of four loop isomers with predominance of the 1:2:1 and 2:1:1 isomers.[36a] Independent work by Patel and co-workers using high-field NMR spectroscopy also showed the predominance of the 1:2:1 loop isomer in the c-*myc* parallel G-quadruplex.[36b] Because neither NMR spectroscopic nor X-ray crystallographic information for the NHE III_1 1:2:1 loop isomer is available, a model was built from the known, closely related X-ray crystal structure of the human intramolecular telomeric G-quadruplex DNA.[17a]

On the basis of the NMR spectroscopic titration of the intermolecular G4A3 quadruplex with **4a**, we propose that **4a** is stacked at the ends of the G-quadruplex at the GT-quadruplex terminus, which is close to the 3′-terminal face of the G-quadruplex. This proposed model is supported by the molecular modeling study of the binding interactions between **4a** and intramolecular G-quadruplex DNA (with a favorable calculated binding energy of $-72.74\ kcal\,mol^{-1}$ (intramolecular G-quadruplex)). We found that an external end-stacking binding mode[41,42] minimizes the energy of structure and shows the best interaction energy and optimum interaction between **4a** and the G-tetrad.

Specificity for G-quadruplex DNA: By using UV/Vis absorption spectroscopy, we first examined the interaction of the platinum(II) complexes with a G-quadruplex-forming oligonucleotide from the promoter region of oncogene c-*myc*. The results showed that the platinum(II) complexes bind to G-quadruplex DNA with binding constants of approximately 10^6–$10^7\ dm^3\,mol^{-1}$, whereas they exhibit only moderate binding to ct-DNA, with K values of 10^4–$10^5\ dm^3\,mol^{-1}$. Moreover, complex **3a** has a 340-fold higher binding affinity towards G-quadruplex DNA from oligonucleotide G4A1 than from dsDNA. Complexes **2** and **4a** also display high selectivity for G-quadruplex DNA, with nearly 75-fold differences in binding values. The competitive dialysis study further confirmed that these complexes selectively bind G-quadruplex DNA over duplex DNA. Notably, the binding constant K values of complex **3a** for G-quadruplex DNA are nearly 100-fold higher than those of the platinum(II) Schiff-base complexes.[28b] The superior selectivity of the platinum(II) complexes with bzimpy or dPzPy scaffolds for G-quadruplex DNA over duplex DNA opens a new avenue for the design of effective G-quadruplex DNA stabilizers.

Stabilization of G-quadruplex DNA: Small molecules that bind to and stabilize the G-quadruplex structure of DNA would be expected to increase the temperature of G-quadruplex dissociation. The extent of G-quadruplex stabilization by the platinum(II) complexes can thus be evaluated by the extent of enhancement of the G-quadruplex melting temperature. The melting of the intramolecular G-quadruplex structure is accompanied by a hypochromicity of the $\lambda =$ 295 nm absorption band.[43] The observed increase in T_m of

the G-quadruplex DNA solution upon addition of **2**, **3a**, **3b**, or **4a** show that all of the platinum(II) complexes in this work can stabilize the G-quadruplex secondary structure of DNA (Table 3).

The specific binding of complexes **1–4** with intramolecular G-quadruplex structures in the promoter region prevents DNA hybridization and subsequent *Thermus aquaticus* (*Taq*) polymerase-mediated DNA extension, the inhibition of which can be used as a measure of the stabilization of G-quadruplex structures. The results from the polymerase stop assays further indicate that all of the platinum(II) complexes used in this study could stabilize the G-quadruplex structure of the c-*myc* sequence in a concentration-dependent manner with IC_{50} values in the range of 2.2–31 μM (Table 4). The IC_{50} values are comparable to those of the quindoline compounds (IC_{50} = 6–36 μM) and 9-*N*-substituted berberine compounds reported in the literature (IC_{50} = 2–7.1 μM).[17] Complex **3a** exhibited the highest inhibitory activity (IC_{50} = 2.21 μM) and is two-fold more potent than the reported Schiff-base complex (IC_{50} = 4.4 μM).[28b] Complex **2** (IC_{50} = 2.59 μM) also displayed high inhibition, suggesting that the introduction of amine side-chains to the bzimpy scaffold helps to stabilize the G-quadruplex. Comparison of the IC_{50} values of **3b** and **3c** with **3a**, and **4b** with **4a**, indicates that the incorporation of the phenylethynyl conjugate group at the R position decreases the activity of these complexes (Table 4). Thus, both the amine side-chain and substituent R of the complexes have direct effects on the potency. Whereas amine side-chains benefit G-quadruplex stabilization, the phenylethynyl conjugate group negatively affects the activity of the complexes.

Inhibition of c-*myc* expression: By measuring the mRNA level of c-*myc* in HepG2 cells, we confirmed the observed effects of platinum(II) complexes on the c-*myc* promoter G-quadruplex. We evaluated whether treatment of HepG2 cells with complexes **1**, **2**, **3a**, and **4a** could interfere with c-*myc* gene expression. The RT-PCR data (Figure 10) showed that **2**, **3a**, and **4a** are potent inhibitors against c-*myc*, whereas **1** was found to be inactive in this assay. In line with the above observations, the result indicates that the amine side-chains could play a pivotal role in the inhibition of c-*myc* transcription. The relatively low potency of **2** compared with **3a** suggests that the amine side-chains could be critical for the potency of the complexes. By modifying the side-chains, new platinum(II) complexes with higher activity against c-*myc* transcription could be developed. However, we do not rule out the possibility that the addition of amine side-chains could improve the bioavailability and thus the biological activities of the complexes.

Molecular light-switch effect: Ethidium bromide is the classical luminescent staining agent used to detect DNA, however, it cannot be used to sense G-quadruplexes. Therefore there is a need to develop luminescent probes that are specific for G-quadruplexes. However, there have been only a few examples of metal-based G-quadruplex DNA probes reported so far. Transition-metal complexes, such as those of ruthenium(II) and platinum(II), have also been documented to bind DNA, and the DNA binding has been known to cause a molecular light-switch effect in a number of cases.[28b,29,30,31a–h] Ideally, a G-quadruplex DNA probe should be highly specific for the quadruplex structure and not duplex DNA. Complex **3b** is weakly emissive in aqueous buffer solution, but displays a strong phosphorescence response upon binding to c-*myc* G-quadruplex DNA, with a 38-fold enhancement at λ_{max}. We found that the increase in emission intensity of **3b** when added to ct-DNA was comparatively much weaker, which suggests that this complex and its derivatives could be developed for the sensitive and selective detection of c-*myc* G-quadruplex DNA. Notably, the emission intensity of **3b** upon binding to G-quadruplex DNA, is five-fold higher than our previously reported platinum(II) Schiff-base complexes. This suggests that these platinum(II) complexes have the potential to function as luminescent staining agents for detection of G-quadruplex DNA in biological samples.

Conclusion

A series of platinum(II) complexes containing bzimpy or dPzPy scaffolds have been synthesized and characterized. Their DNA and G-quadruplex binding properties, and their impact on the regulation of c-*myc* oncogene were evaluated by polymerase stop assay, NMR spectroscopic titration experiments, molecular modeling, competitive dialysis, UV melting studies, spectroscopic titrations, and RT-PCR assays. A platinum(II) complex containing bzimpy ligand was the initial hit complex that exhibited moderate stabilization of G-quadruplex DNA. By means of in silico hit-to-lead optimization docking, superior candidate complexes containing amine side-chains introduced to bzimpy or dPzPy scaffold were synthesized. These new platinum(II) complexes were found to display superior selectivity towards c-*myc* G-quadruplex DNA and not duplex DNA. They showed significant inhibition of c-*myc* gene transcription in cultured cells, presumably through the stabilization of the G-quadruplex structure. A structure-guided activity concept for the stabilization of the G-quadruplex DNA structure in the NHE III_1 sequence based on the molecular docking has been demonstrated. The structure–activity relationships determined in this study may potentially serve as the basis of future rational design of metal-based drugs that target the G-quadruplex.

Experimental Section

Materials: DNA oligomers G4A1, G4A1-rev, G4A2, G4A3, c-*myc* S, c-*myc* A, β-actin S, and β-actin A (listed in Table 6) were obtained from Tech Dragon (Hong Kong, P.R. China). The DNA concentration per pair was determined based on the absorbance value at λ = 260 nm (ε_{260} = 3.81×10^5 M (strand)$^{-1}$ cm^{-1} for G4A1 by using UV/Vis absorption spectroscopy. Unless otherwise stated, spectroscopic titration experiments

Table 6. Sequences of oligomers (primers) used in the present study.

Oligomer	Sequence
G4A1	5′-TGGGGAGGGTGGGGAGGGTGGGGAAGG-3′
G4A1-rev	5′-ATCGATCGC TTCTCGTCCTTCCCCA-3′
G4A2	5′-TGGGGAGGGTGGAAAGGGTGGGGAAGG-3′
G4A3	5′-TGAGGGTGGIGAGGGTGGGGAAGG-3′
c-*myc* A	5′-TGGTGCTCCATGAGGAGACA-3′
c-*myc* S	5′-GTGGCACCTCTTGAGGACCT-3′
β-actin A	5′-GTTGCTATCCAGGCTGTGC-3′
β-actin S	5′-GCATCCTGTCGGCAATGC-3′

were performed in 10 mM Tris/HCl (pH 7.4) containing 100 mM KCl. SuperScript II Reverse Transcriptase was purchased from Invitrogen. *Taq* polymerase and the total RNA isolation kit (RNeasy mini kit) were purchased from QIAGEN. Stock solutions of all the derivatives (10 mM) were made in DMSO (10%) or double-distilled water. Further dilutions to working concentrations were made with double-distilled water.

Synthesis: 2,6-Bis(benzimidazol-2-yl)pyridine (bzimpy),[33] 2,6-bis(pyrazol-3-yl)pyridine (dPzPy),[34] 3-morpholinyl-1-chloropropane,[44] and 1-(3-chloro-propyl)-piperidine[44] were synthesized and characterized according to reported methods.

2,6-Bis[1-(3-morpholinopropyl)-1*H*-benzo[*d*]imidazol-2-yl]pyridine (L1): Solid NaH (230 mg, 6 mmol) was added to a solution of bzimpy (622 mg, 2 mmol) and NaI (1.50 g, 10 mmol) in anhydrous DMF (10 mL). When H_2 evolution was complete, the reaction mixture was warmed to 50 °C and stirred under Ar for 2 h. 3-Morpholinyl-1-chloropropane (982 mg, 6 mmol) was introduced into the reaction system and the reaction was stirred overnight at RT. A solution of aqueous NH_4Cl (10%) was added at 0 °C, and the reaction was stirred vigorously for 30 min. The mixture was extracted with dichloromethane and washed successively with water (3×10 mL) and brine. The organic fractions were dried over Na_2SO_4 and the solvent was removed under reduced pressure. The resulting oil was purified by column chromatography to afford the title product as a pale yellow oil (390 mg, 35%). ^{1}H NMR ($CDCl_3$, 400 MHz): δ=8.32 (d, J=7.5 Hz, 2H), 8.05 (t, J=7.8 Hz, 1H), 7.87 (d, J=8.0 Hz, 2H), 7.51 (d, J=6.8 Hz, 2H), 7.377.32 (m, 4H), 4.78 (t, J=6.9 Hz, 4H), 3.43–3.41 (m, 8H), 2.10–2.07 (m, 12H), 1.91–1.85 ppm (m, 4H); ^{13}C NMR (100 MHz, $CDCl_3$): δ=150.1, 149.9, 142.6, 138.2, 136.3, 125.4, 123.6, 122.9, 120.3, 110.4, 66.6, 55.3, 53.3, 42.9, 26.5 ppm; HRMS (EI): *m*/*z* calcd for $C_{33}H_{39}N_7O_2$: 565.3165 $[M]^+$; found: 565.3164.

2,6-Bis[1-(3-piperidinepropyl)-1*H*-benzo[*d*]imidazol-2-yl]pyridine (L2): This compound was synthesized by using a similar procedure to **L1** except that 1-(3-chloropropyl)piperidine was used in place of 3-morpholinyl-1-chloropropane. Yield: 34%. ^{1}H NMR (400 MHz, $CDCl_3$): δ=8.32 (d, J=7.5 Hz, 2H), 8.06 (t, J=7.8 Hz, 1H), 7.87 (d, J=8.0 Hz, 2H), 7.54 (d, J=6.8 Hz, 2H), 7.35–7.26 (m, 4H), 4.78 (t, J=6.9 Hz, 4H), 2.09–2.04 (m, 12H), 1.94–1.87 (m, 4H), 1.34–1.26 ppm (m, 12H); HRMS (EI): *m*/*z* calcd for $C_{35}H_{43}N_7$: 561.3580 $[M]^+$; found: 561.3582.

2,6-Bis[1-(3-morpholinopropyl)-1*H*-pyrazol-3-yl]pyridine (L3): This compound was synthesized by using a similar procedure to **L1**, except that dPzPy was used in place of bzimpy. Yield: 65%. ^{1}H NMR ($CDCl_3$, 400 MHz): δ=8.31 (t, J=7.8 Hz, 2H), 8.04 (t, J=7.6 Hz, 1H), 7.88–7.85 (m, 2H), 7.52–7.50 (m, 2H), 4.78 (t, J=6.6 Hz, 4H), 3.49–3.41 (m, 8H), 2.10–2.01 (m, 12H), 1.90–1.85 ppm (m, 4H); ^{13}C NMR ($CDCl_3$, 100 MHz): δ=150.2, 149.9, 142.7, 136.3, 120.4, 110.4, 66.6, 55.4, 53.4, 42.9, 26.6 ppm; HRMS (EI): *m*/*z* calcd for $C_{25}H_{35}N_7O_2$: 465.2852 $[M]^+$; found: 465.2851.

Compound 1: Bzimpy (311 mg, 1 mmol) and $[Pt(DMSO)_2Cl_2]$ (421 mg, 1 mmol) was dissolved in $CHCl_3$ (12 mL), and the mixture was heated to reflux and stirred for 24 h. The solution turned orange-yellow. The reaction was filtered and the filtrate was concentrated to 4 mL under reduced pressure. Excess Et_2O was added to precipitate a pale yellow solid that was washed with Et_2O and redissolved in DMF (4 mL), then excess NaOTf (0.5 g) was added. The solution was stirred for 48 h at RT and excess Et_2O was added. The precipitated solid was washed with water and Et_2O and dried in air to afford the title product as a pale yellow solid (660 mg, 72%). ^{1}H NMR ([D$_6$]DMSO, 400 MHz): δ=8.08–8.04 (m, 1H), 7.97–7.93 (m, 2H), 7.81–7.75 (m, 2H), 7.56 (t, J=8.0 Hz, 2H), 7.23–7.17 ppm (m, 4H); FAB-MS: *m*/*z*: 541 $[M]^+$; elemental analysis calcd (%) for $C_{20}H_{13}ClF_3N_5O_3PtS$: C 34.77, H 1.90, N 10.14; found: C 34.53, H 1.87, N 10.27.

Compound 2: The synthesis of **2** was similar to that of **1**, except that 2,6-bis[1-(3-morpholinopropyl)-1*H*-benzo[*d*]imidazol-2-yl]pyridine was used. Yield: 699 mg, 76%. ^{1}H NMR ([D$_6$]DMSO, 400 MHz): δ=8.58 (t, J=11.2 Hz, 1H) , 8.50 (d, J=8.0 Hz, 2H), 8.10 (s, 2H), 7.74 (d, J=10.0 Hz, 2H), 7.50 (J=8.5 Hz, 2H), 7.48 (J=10.0 Hz, 2H), 4.63–4.46 (m, 4H), 2.53–2.24 (m, 12H), 1.86–1.73 ppm (m, 12H); FAB-MS: *m*/*z*: 795 $[M]^+$; elemental analysis calcd (%) for $C_{34}H_{39}ClF_3N_7O_5PtS$: C 43.20, H 4.16, N 10.37; found: C 43.13, H 4.07, N 10.49.

Compound 3a: The synthesis of **3a** was similar to that of **1** except that 2,6-bis[1-(3-piperidinepropyl)-1*H*-benzo[*d*]imidazol-2-yl]pyridine was used. Yield: 761 mg, 81%. ^{1}H NMR ([D$_6$]DMSO, 400 MHz): δ=8.55 (t, J=11.2 Hz, 1H) , 8.47 (d, J=8.0 Hz, 2H), 8.06 (s, 2H), 7.70 (d, J=10.0 Hz, 2H), 7.50 (t, J=8.5 Hz, 2H), 7.43 (d, J=10.0 Hz, 2H), 4.60–4.36 (m, 4H), 2.49–2.28 (m, 16H), 1.23–1.05 ppm (m, 12H); FAB-MS: *m*/*z*: 792 $[M]^+$; elemental analysis calcd (%) for $C_{36}H_{43}ClF_3N_7O_5PtS$: C 45.93, H 4.60, N 10.42; found: C 45.88, H 4.57, N 10.65.

Compound 3b: Ethynylbenzene (0.3 mmol), CuI and anhydrous Et_3N (0.5 mL) were added to a solution of complex **3a** (0.15 mmol) in DMF (10 mL). The mixture was stirred at RT for 12 h under argon, and then filtered. Excess Et_2O was then added to precipitate pale yellow solid, which was washed with Et_2O and dried in air to afford the title product (102 mg, 79%). ^{1}H NMR ([D$_6$]DMSO, 400 MHz): δ=8.49–8.35 (m, 3H), 7.93 (s, 1H), 7.60 (s, 3H), 7.48 (d, J=10.0 Hz, 4H), 7.35–7.28 (m, 2H), 7.19–7.04 (m, 3H), 4.76–4.63 (brs, 4H), 2.87 (s, 2H), 2.71 (s, 2H), 2.48–2.35 (m, 10H), 1.69–1.17 ppm (m, 14H); FAB-MS: *m*/*z*: 857 $[M]^+$; elemental analysis calcd (%) for $C_{44}H_{48}F_3N_7O_3PtS$: C 52.48, H 4.80, N 9.74; found: C 52.43, H 4.77, N 9.82.

Compound 3c: The synthesis of **3c** was similar to that of **3b** except that 4-ethynylphenoxy-2,3,4,6-tetra-*O*-acetyl-β-D-glucopyranoside was used. Yield: 69%.^{1}H NMR ([D$_6$]DMSO, 300 MHz): δ=8.68–8.43 (m, 4H), 7.83 (d, J=7.8 Hz, 2H), 7.56 (d, J=4.8 Hz, 4H), 7.36 (d, J=6.0 Hz, 2H), 7.23 (d, J=7.2 Hz, 1H), 7.08 (d, J=7.5 Hz, 2H), 6.85 (d, J=6.3 Hz, 1H), 5.49–5.17 (m, 6H), 4.75–4.73 (m, 2H), 4.43 (d, J=4.8 Hz, 2H), 4.11–4.05 (m, 4H), 2.46 (s, 24H), 2.20–1.91 ppm (m, 12H); FAB-MS: *m*/*z*: 1205 $[M]^+$; elemental analysis calcd (%) for $C_{58}H_{66}F_3N_7O_{13}PtS$: C 51.48, H 4.92, N 7.24; found: C 50.91, H 4.72, N 7.36.

Compound 4a: The synthesis of **4a** was similar to that of **1**, except that 2,6-bis[1-(3-morpholinopropyl)-1*H*-pyrazol-3-yl]pyridine was used. Yield: 85%. ^{1}H NMR ($CDCl_3$, 400 MHz): δ=8.37 (t, J=7.9 Hz, 1H), 8.19–8.14 (m, 4H), 7.35 (d, J=2.8 Hz, 2H), 4.76 (d, J=6.4 Hz, 4H), 3.73–3.71 (m, 8H), 2.46 (s, 8H), 2.39–2.36 (m, 4H), 2.13–2.05 ppm (m, 4H); ^{13}C NMR ($CDCl_3$, 100 MHz): δ=154.2, 149.2, 143.8, 137.9, 120.9, 108.5, 66.8, 54.6, 53.6, 51.4, 27.0 ppm; FAB-MS: *m*/*z*: 695 $[M]^+$; elemental analysis calcd (%) for $C_{26}H_{35}ClF_3N_7O_5PtS$: C 36.95, H 4.17, N 11.60; found: C 36.83, H 4.14, N 11.77.

Compound 4b: The synthesis of **4b** was similar to that of **3b**, except that **4a** was used. Yield: 82%. ^{1}H NMR ([D$_6$]DMSO, 400 MHz): δ=8.37 (d, J=8.0 Hz, 1H) , 8.16 (d, J=10.0 Hz, 1H), 7.76–7.55 (m, 2H), 7.36 (d, J=6.0 Hz, 2H), 7.27–7.02 (m, 6H), 4.84 (t, J=10.0 Hz, 4H), 3.50–3.43 (m, 8H), 2.27 (s, 4H), 2.18 (s, 4H), 2.17–2.02 ppm (m, 8H); FAB-MS: *m*/*z*: 761 $[M]^+$; elemental analysis calcd (%) for $C_{34}H_{40}F_3N_7O_5PtS$: C 44.83, H 4.43, N 10.76; found: C 44.75, H 4.41, N 10.84.

Absorption titration: Solutions of the platinum(II) complexes (50 μM) were prepared in Tris/HCl (10 mM, pH 7.4) that contained KCl buffer (100 mM) and aliquots of a millimolar stock solution of G4A1 DNA were added. Absorption spectra were recorded in the λ=200–550 nm spectral range, after equilibration at 20 °C for 10 min.

Emission Titration: Solutions of the platinum(II) complexes (50 μM) were prepared in 10 mM Tris/HCl (pH 7.4) containing 100 mM KCl buffer and aliquots of a millimolar stock of G4A1 DNA or ct-DNA solution (0–200 μM) were added. Emission spectra were recorded in the λ=500–

800 nm range after equilibration at 20 °C for 10 min per aliquot until saturation point had been reached.

UV melting study: The c-*myc* G-quadruplex sample was prepared by heating the oligonucleotides in Tris/HCl buffer (10 mM, pH 7.4, EDTA (1 mM), and KCl (100 mM)) followed by slow cooling. The melting profile of c-*myc* quadruplex (20 μM) was recorded in the absence and presence of 20 μM complexes **2**, **3a**, **3b**, and **4a** by using a Perkin–Elmer spectrophotometer equipped with a thermostatically controlled cell holder with a heating rate of 1 °C min^{-1}. Data were collected at $\lambda = 295$ nm. T_m was calculated as the mid-point of the absorbance curve.

Competition dialysis experiment: Competition dialysis experiments were performed as described.[45] A Tris/HCl buffer (10 mM, pH 7.4) that contained NaCl (100 mM) was used for all experiments. For each competition dialysis assay, the test ligands (10 μM) were dialyzed against the nucleic acid array. An aliquot of each of the DNA samples (0.2 mL, 45 μM monomeric unit) was pipetted into a separate 0.2 mL mini dialysis kit unit with a 1000 molecular-weight cutoff tubing (GE Healthcare, Piscataway, New Jersey, USA). The entire dialysis units were then placed in the beaker containing the dialysate solution. At the end of the 24 h equilibration period at RT, DNA samples were carefully removed to microfuge tubes and sodium dodecyl sulfate (SDS) was added to a final concentration of 1% (w/v). The total concentration of ligand (C_t) within each dialysis tube was then measured spectrophotometrically at $\lambda = 336$ nm with an extinction coefficient of 10250 M^{-1} cm^{-1} for **2**, $\lambda = 325$ nm with an extinction coefficient of 15200 M^{-1} cm^{-1} for **3a** and at $\lambda = 316$ nm with an extinction coefficient of 8336 M^{-1} cm^{-1} for **4a**. The free ligand concentration (C_f) was determined spectrophotometrically by using an aliquot of the dialysate solution. The amount of bound ligand was determined by the difference between the total ligand concentration and the free ligand concentration ($C_b = C_t - C_f$). Final analysis of the data was carried out using the Origin 6.0 software (OriginLab, Northampton, Massachusetts, USA).

NMR spectroscopy: The NMR spectroscopic titration experiment was conducted in phosphate buffer (H_2O/D_2O 90:10 with KCl (150 mM), KH_2PO4 (25 mM), EDTA (1 mM); pH 7.0). G4A3 quadruplex DNA in buffer was titrated with platinum(II) complex (10 μM) in [D_6]DMSO. The spectra were recorded by using a 600 MHz Bruker spectrometer at 25 °C.

Polymerase stop assay: The polymerase stop assay was performed as described previously.[17] The reactions were performed in 10×PCR buffer that contained 10 μM of each pair of oligomers, dNTP (10 mM), *Taq* polymerase (2.5 U), and the indicated concentrations of the complexes. Reaction mixtures were incubated in a thermocycler at 95 °C for 3 min, followed by 30 cycles of 95 °C for 15 s, 58 °C for 30 s, and 72 °C for 30 s. Amplified products were resolved on 30% nondenaturing polyacrylamide gels in 1×TBE and stained with SYBN (1:1000).

Molecular modeling: A model study on the stacking interaction between platinum(II) complex and G-quadruplex DNA was performed. This was done by using Gaussian 03. The platinum complex was optimized by using DFT with a LanL2MB basis set.[46] The optimized structure of the platinum complex was used to do the docking. Molecular docking was performed by using the ICM-Pro 3.6-1d program (Molsoft).[37] According to ICM method, the molecular system was described by using internal coordinates as variables. Energy calculations were based on the ECEPP/3 force field with a distance-dependent dielectric constant. The biased-probability Monte Carlo (BPMC) minimization procedure was used for global energy optimization. The BPMC global energy optimization method consists of the following steps: 1) a random conformation change in the free variables according to a predefined continuous probability distribution; 2) local energy minimization of analytical differentiable terms; 3) calculation of the complete energy including non-differentiable terms, such as entropy and solvation energy; 4) acceptance or rejection of the total energy based on the Metropolis criterion and return to step 1. The binding between platinum(II) complex and DNA was evaluated by using binding energy, including grid energy, continuum electrostatic, and entropy terms. The initial models of loop isomers A and B were built from the X-ray crystal structures of human intramolecular telomeric G-quadruplex (PDB code: 1KF1),[32] according to a previously reported procedure. Hydrogen and missing heavy atoms were added to the receptor structure, followed by local minimization by using the conjugate gradient algorithm and analytical derivatives in the internal coordinates. In the docking analysis, the binding site was assigned across the entire structure of the DNA molecule. The ICM docking was performed to find the most favorable orientation. The resulting platinum(II) complex–G-quadruplex DNA trajectories were energy minimized, and the interaction energies were computed.

Cell culture: Human normal lung fibroblast (CCD-19Lu), human hepatocarcinoma (HepG2), and human cervical epithelioid cancer (HeLa) were obtained from the American Type Culture Collection (Rockville, MD). Human nasopharyngeal carcinoma cells (SUNE1) were generously provided by Prof. S. W. Tsao (Department of Anatomy, The University of Hong Kong). The cell lines were maintained in cell culture media (minimum essential medium for CCD-19Lu, HepG2, and HeLa; RPMI-1640 medium for SUNE1) supplemented with fetal bovine serum (10%), penicillin (100 U mL^{-1}), and streptomycin (100 μg mL^{-1}) at 37 °C under a humidified atmosphere with 5% CO_2.

Reverse transcriptase–polymerase chain reaction (RT-PCR): HepG2 cells were grown in six-well plates for 24 h. The cells were treated with the indicated concentrations of Pt^{II} complexes. Treated and untreated cells were harvested after 16 h. Total RNA was extracted according to the manufacturer's instruction. Reverse transcription was carried out by incubating RNA (1 μg), random primers (100 ng), and dNTPs (0.5 mM) at 42 °C for 5 min, followed by a further incubation with 200 units of SuperScript II reverse transcriptase in 1×First-Strand buffer at 42 °C for 30 min for reverse transcription and then at 95 °C for 3 min to inactivate the enzyme. PCRs (containing cDNA (1 μg), 10 mM of dNTPs, of *Taq* DNA polymerase (2.5 U), 10×PCR buffer and 10 μM of each primer) were performed for 22 cycles, consisting of 15 s at 95 °C, 30 s at 58 °C, and 30 s at 72 °C in a thermocycler. The samples were heated for 5 min at 95 °C before the first cycle, and the extension time was lengthened to 5 min during the last cycle. PCR products were size-fractionated on a 1.2% agarose gel.

Cytotoxicity test: MTT cell-viability assays were conducted in 96-well, flat-bottomed microtiter plates. Cells were seeded in a 96-well microplate at 2000 cells per well in growth medium solution (150 μL). Complexes **1**–**4** and cisplatin (positive control) were dissolved in DMSO and mixed with the growth medium (final concentration 1% DMSO). Drug-treated and untreated cells were incubated for 8 d at 37 °C, 5% CO_2 in a humidified incubator. MTT reagent was added to each well. The microplates were then reincubated at 37 °C in 5% CO_2 for 4 h, prior to the addition of solubilization solution (10% SDS in 0.01 M HCl). The microplates were further incubated for 24 h. Absorbances at $\lambda = 550$ nm were measured on a microplate reader. IC_{50} values (concentration required to reduce the absorbance by 50% compared with the controls) for each complex were determined by the dose dependence of surviving cells after exposure to the platinum(II) complexes for 8 d.

Acknowledgements

We are grateful for financial support from The University of Hong Kong (University Development Fund), the Hong Kong Research Grant Council (HKU 7052/07P), and the Areas of Excellence Scheme established under the University Grants Committee of the Hong Kong Special Administrative Region, China (AoE/P-10/01).

[1] L. H. Hurley, *Nat. Rev. Cancer* **2002**, *2*, 188.
[2] X. L. Yang, A. H. Wang, *Pharmacol. Ther.* **1999**, *83*, 181.
[3] U. Pindur, G. Fischer, *Curr. Med. Chem.* **1996**, *3*, 379.
[4] J. T. Davis, *Angew. Chem.* **2004**, *116*, 684; *Angew. Chem. Int. Ed.* **2004**, *43*, 668.
[5] C. A. Spencer, M. Groudine, *Adv. Cancer Res.* **1991**, *56*, 1.
[6] K. B. Marcu, S. A. Bossone, A. J. Patel, *Annu. Rev. Biochem.* **1992**, *61*, 809.
[7] L. M. Facchini, L. Z. Penn, *FASEB J.* **1998**, *12*, 633.

[8] a) S. Pelengaris, B. Rudolph, T. Littlewood, *Curr. Opin. Genet. Dev.* **2000**, *10*, 100; b) D. J. Patel, A. T. Phan, V. Kuryavyi, *Nucleic Acids Res.* **2007**, *35*, 7429.
[9] a) E. F. Michelotti, T. Tomonaga, H. Krutzsch, D. Levens, *J. Biol. Chem.* **1995**, *270*, 9494; b) T. Tomonaga, D. Levens, *Proc. Natl. Acad. Sci. USA* **1996**, *93*, 5830.
[10] a) T. Simonsson, P. Pecinka, M. Kubista, *Nucleic Acids Res.* **1998**, *26*, 1167; b) T. Simonsson, M. Pribylova and M. Vorlickova, *Biochem. Biophys. Res. Commun.* **2000**, *278*, 158.
[11] a) E. H. Postel, S. J. Berberich, J. W. Rooney, D. M. Kaetzel, *J. Bioenerg. Biomembr.* **2000**, *32*, 277; b) A. Ambrus, D. Chen, J. Dai, R. A. Jones, D. Yang, *Biochemistry* **2005**, *44*, 2048.
[12] D. Sun, B. Thompson, B. E. Cathers, M. Salazar, S. M. Kerwin, J. O. Trent, T. C. Jenkins, S. Neidle, L. H. Hurley, *J. Med. Chem.* **1997**, *40*, 2113.
[13] T. Lemarteleur, D. Gomez, R. Paterski, E. Mandine, P. Mailliet, J. F. Riou, *Biochem. Biophys. Res. Commun.* **2004**, *323*, 802.
[14] C. L. Grand, H. Han, R. M. Munoz, S. Weitman, D. D. Von Hoff, L. H. Hurley, D. J. Bearss, *Mol. Cancer Ther.* **2002**, *1*, 565.
[15] J. Seenisamy, S. Bashyam, V. Gokhale, H. Vankayalapati, D. Sun, A. Siddiqui-Jain, N. Streiner, K. Shin-ya, E. White, W. D. Wilson, L. H. Hurley, *J. Am. Chem. Soc.* **2005**, *127*, 2944.
[16] A. Rangan, O. Y. Fedoroff, L. H. Hurley, *J. Biol. Chem.* **2001**, *276*, 4640.
[17] a) T. M. Ou, Y. J. Lu, C. Zhang, Z. S. Huang, X. D. Wang, J. H. Tan, Y. Chen, D. L. Ma, K. Y. Wong, J. C. O. Tang, A. S. C. Chan, L. Q. Gu, *J. Med. Chem.* **2007**, *50*, 1465; b) Y. J. Lu, T. M. Ou, J. H. Tan, J. Q. Hou, W. Y. Shao, D. Peng, N. Sun, X. D. Wang, W. B. Wu, Z. S. Huang, D. L. Ma, K. Y. Wong, L. Q. Gu, *J. Med. Chem.* **2008**, *51*, 6381; c) Y. Ma, T. M. Ou, J. Q. Hou, Y. J. Lu, J. H. Tan, L. Q. Gu, Z. S. Huang, *Bioorg. Med. Chem.* **2008**, *16*, 7582.
[18] R. T. Wheelhouse, D. Sun, H. Han, F. X. Han, L. H. Hurley, *J. Am. Chem. Soc.* **1998**, *120*, 3261.
[19] R. J. Harrison, S. M. Gowan, L. R. Kelland, S. Neidle, *Bioorg. Med. Chem. Lett.* **1999**, *9*, 2463.
[20] a) S. Redon, S. Bombard, M. A. Elizondo-Riojas, J. C. Chottard, *Biochemistry* **2001**, *40*, 8463; b) W. Tuntiwechapikul, M. Salazar, *Biochemistry* **2001**, *40*, 13652; c) I. V. Smirnov, F. W. Kotch, I. J. Pickering, J. T. Davis, R. H. Shafer, *Biochemistry* **2002**, *41*, 12133; d) L. R. Keating, V. A. Szalai, *Biochemistry* **2004**, *43*, 15891.
[21] A. Maraval, S. Franco, C. Vialas, G. Pratviel, M. A. Blasco, B. Meunier, *Org. Biomol. Chem.* **2003**, *1*, 921.
[22] a) I. M. Dixon, F. Lopez, J. P. Estève, A. M. Tejera, M. A. Blasco, G. Pratviel, B. Meunier, *ChemBioChem* **2005**, *6*, 123; b) I. M. Dixon, F. Lopez, A. M. Tejera, J. P. Estève, M. A. Blasco, G. Pratviel, B. Meunier, *J. Am. Chem. Soc.* **2007**, *129*, 1502.
[23] a) H. Bertrand, D. Monchaud, A. De Cian, R. Guillot, J. L. Mergny, M. P. Teulade-Fichou, *Org. Biomol. Chem.* **2007**, *5*, 2555; b) H. Bertrand, S. Bombard, D. Monchaud, M. P. Teulade-Fichou, *J. Biol. Inorg. Chem.* **2007**, *12*, 1003.
[24] S. E. Evans, M. A. Mendez, K. B. Turner, L. R. Keating, R. T. Grimes, S. Melchoir, V. A. Szalai, *J. Biol. Inorg. Chem.* **2007**, *12*, 1235.
[25] a) A. Arola-Arnal, J. Benet-Buchholz, S. Neidle, R. Vilar, *Inorg. Chem.* **2008**, *47*, 11910; b) S. Shi, J. Liu, T. Yao, X. Geng, L. Jiang, Q. Yang, L. Cheng, L. Ji, *Inorg. Chem.* **2008**, *47*, 2910.
[26] R. Kieltyka, J. Fakhoury, N. Moitessier, H. F. Sleiman, *Chem. Eur. J.* **2008**, *14*, 1145.
[27] a) J. E. Reed, A. A. Arnal, S. Neidle, R. Vilar, *J. Am. Chem. Soc.* **2006**, *128*, 5992; b) J. E. Reed, A. J. P. White, S. Neidle, R. Vilar, *Dalton Trans.* **2009**, 2558.
[28] a) D. L. Ma, C. M. Che, S. C. Yan, *J. Am. Chem. Soc.* **2009**, *131*, 1835; b) P. Wu, D. L. Ma, C. H. Leung, S. C. Yan, N. Zhu, R. Abagyan, C. M. Che, *Chem. Eur. J.* **2009**, *15*, 13008.
[29] J. Alzeer, B. R. Vummidi, P. J. C. Roth, N. W. Luedtke, *Angew. Chem.* **2009**, *121*, 9526; *Angew. Chem. Int. Ed.* **2009**, *48*, 9362.
[30] a) C. M. Che, M. Yang, K. H. Wong, H. L. Chan, *Chem. Eur. J.* **1999**, *5*, 3350; b) H. L. Chan, D. L. Ma, M. Yang, C. M. Che, *ChemBioChem* **2003**, *4*, 62; c) D. L. Ma, C. M. Che, *Chem. Eur. J.* **2003**, *9*, 6133; d) D. L. Ma, T. Y. T. Shum, F. Zhang, C. M. Che, M. Yang, *Chem. Commun. (Cambridge)* **2005**, 4675.
[31] a) C. Hiort, P. Lincoln, B. Norden, *J. Am. Chem. Soc.* **1993**, *115*, 3448; b) C. J. Murphy, J. K. Barton, *Methods Enzymol.* **1993**, *226*, 576; c) H. Q. Liu, T. C. Cheung, C. M. Che, *Chem. Commun.* **1996**, 1039; d) K. E. Erkkila, D. T. Odom, J. K. Barton, *Chem. Rev.* **1999**, *99*, 2777; e) S. A. Tysoe, R. Kopelman, D. Schelzig, *Inorg. Chem.* **1999**, *38*, 5196; f) B. M. Zeglis, V. C. Pierre, J. K. Barton, *Chem. Commun. (Cambridge)* **2007**, 4565; g) C. A. Mitsopoulou, C. E. Dagas, C. Makedonas, *J. Inorg. Biochem.* **2008**, *102*, 77; h) Y. M. Chen, Y. J. Liu, Q. Li, K. Z. Wang, *J. Inorg. Biochem.* **2009**, *103*, 1395; i) D. L. Ma, W. L. Wong, W. H. Chung, F. Y. Chan, P. K. So, T. S. Lai, Z. Y. Zhou, Y. C. Leung, K. Y. Wong, *Angew. Chem.* **2008**, *120*, 3795; *Angew. Chem. Int. Ed.* **2008**, *47*, 3735.
[32] G. N. Parkinson, M. P. H. Lee, S. Neidle, *Nature* **2002**, *417*, 876.
[33] S. M. Yue, H. B. Xu, J. F. Ma, Z. M. Su, Y. H. Kan, H. J. Zhang, *Polyhedron* **2006**, *25*, 635.
[34] a) A. K. Pleier, H. Glas, M. Grosche, P. Sirsch, W. R. Thiel, *Synthesis* **2001**, 55; b) P. Gamez, R. H. Steensma, W. L. Driessen, J. Reedijk, *Inorg. Chim. Acta* **2002**, *333*, 51.
[35] a) Q. Z. Yang, L. Z. Wu, Z. X. Wu, L. P. Zhang, C. H. Tung, *Inorg. Chem.* **2002**, *41*, 5653; b) K. M. C. Wong, W. S. Tang, B. W. K. Chu, N. Zhu, V. W. W. Yam, *Organometallics* **2004**, *23*, 3459; c) V. G. Vaidyanathan, B. U. Nair, *Eur. J. Inorg. Chem.* **2005**, 3756; d) A. Y. Y. Tam, W. H. Lam, K. M. C. Wong, N. Y. Zhu, V. W. W. Yam, *Chem. Eur. J.* **2008**, *14*, 4562.
[36] a) J. Seenisamy, E. M. Rezler, T. J. Powell, D. Tye, V. Gokhale, C. S. Joshi, A. Siddiqui-Jain, L. H. Hurley, *J. Am. Chem. Soc.* **2004**, *126*, 8702; b) A. T. Phan, Y. S. Modi, D. J. Patel, *J. Am. Chem. Soc.* **2004**, *126*, 8710.
[37] a) M. Totrov, R. Abagyan, *Proteins: Struct., Funct., Genet.* **1997**, *29 (Suppl 1)*, 215; b) D. L. Ma, T. S. Lai, F. Y. Chan, W. H. Chung, R. Abagyan, Y. C. Leung, K. Y. Wong, *ChemMedChem* **2008**, *3*, 881.
[38] F. X. Han, R. T. Wheelhouse, L. H. Hurley, *J. Am. Chem. Soc.* **1999**, *121*, 3561.
[39] C. V. Kumar, E. H. Asuncion, *J. Am. Chem. Soc.* **1993**, *115*, 8547.
[40] A. T. Phan, V. Kuryavyi, H. Y. Gaw, D. J. Patel, *Nat. Chem. Biol.* **2005**, *1*, 167.
[41] S. M. Haider, G. N. Parkinson, S. Neidle, *J. Mol. Biol.* **2003**, *326*, 117.
[42] M. A. Read, S. Neidle, *Biochemistry* **2000**, *39*, 13422.
[43] J. L. Mergny, A. T. Phan, L. Lacroix, *FEBS Lett.* **1998**, *435*, 74.
[44] C. Le Sann, J. Huddleston, J. Mann, *Tetrahedron* **2007**, *63*, 12903.
[45] P. Ragazzon, J. B. Chaires, *Methods* **2007**, *43*, 313.
[46] a) P. J. Hay, W. R. Wadt, *J. Chem. Phys.* **1985**, *82*, 270; b) W. R. Wadt, P. J. Hay, *J. Chem. Phys.* **1985**, *82*, 284; c) P. J. Hay, W. R. Wadt, *J. Chem. Phys.* **1985**, *82*, 299.

Received: January 21, 2010
Published online: April 30, 2010

